3-D modelling of single-lap multi-bolted joints under quasi-static conditions

Khairi Supar, and Hilton Ahmad

Citation: AIP Conference Proceedings **1885**, 020020 (2017); doi: 10.1063/1.5002214

View online: http://dx.doi.org/10.1063/1.5002214

View Table of Contents: http://aip.scitation.org/toc/apc/1885/1

Published by the American Institute of Physics

3-D Modelling of Single-lap Multi-bolted Joints under Quasi-static Conditions

Khairi Supar[1,a)] and Hilton Ahmad[1,b)]

[1]*Faculty of Civil and Environmental Engineering, Universiti Tun Hussein Onn Malaysia, 86400 Parit Raja, Batu Pahat, Johor Darul Ta'zim. Malaysia*

Corresponding author: [a)]khairisupar@gmail.com
[b)]hilton@uthm.edu.my

Abstract. Multi-bolted joint configurations are commonly used in joining different parts in various engineering sectors, ability of bolts to transfer by-pass stress to adjacent bolts prone of net-tension to occur compared to single-bolt joint configurations. There is bearing-bypass envelope has been proposed but due to complexities in bearing damage leading to difficulties in predicting failure modes. More recently, strength prediction works in composite structures are carried out within finite element framework to take into advantage of advanced computing technology. Current work implemented a three-dimensional Extended Finite Element Method (XFEM) framework of single-row multi-bolted joints to predict the bearing stress at failure, validated against experimental datasets. A testing series comprised of different clamping load and number of bolts in a single row. All testing series failed in net-tension failure mode, suggesting prominent effect from stress concentration. Crack initiation and propagations shows similarity within XFEM and experimental observations. Good agreements were found (less than 10% discrepancy) due to ability in 3-D modelling to capture effect of bolt load and frictional load transfer.

INTRODUCTION

Materials engineers and scientists worldwide are chasing to produce an engineering material that is not only light but has excellent mechanical properties. One class of advanced engineering materials is known as "composite materials" comprised of reinforcing fibers and matrix binder that is formerly used in aircraft and automotive industries, but as a result of price drop over last four decades, these materials were implemented in manufacturing, civil engineering applications and defence sectors. Commercially used reinforcing fibers are carbon, glass and aramid fibers but these synthetic fibers require mineral coring and associated to human health hazards. Nishino, Hirao and Kotera [1] has reported that kenaf fibers possess excellent modulus of elasticity and elongation at break. Natural fibers such as kenaf fibers are renewable, has good thermal and acoustic insulations, and less hazardous during handling process. drilling holes, and due to plate discontinuity, stress concentration is prone to occur and reduce the loading capacity of the respective plates. Anders and Ahmad [2] has carried out experimental work on notched plate problem and found that notched strength is largely dependent upon hole size, plate thickness and plate lay-ups. However, in bolted joint problems, bearing strength at failures exhibited much more complex damage mechanisms as three primary failure modes may occur dependent upon clamping load, lay-up types and friction coefficient. Single-lap joint is the most prominent joint types, however due to unsymmetrical loading path subjected to secondary bending occurrence. This increased the tensile stress at the vicinity of the hole edge and reduce its loading capacity. Effect of secondary bending is significant with dissimilar joining plates with higher relative material modulus.

In multi-bolted joints, there is an interaction between bearing stress and by-pass loading transferred to adjacent bolts. Crews and Naik [3] initially proposed bearing-bypass interaction envelope for CFRP and later by Hung and Chang [4] proposed damage accumulation model to predict composite joints strength as subjected to bi-axial by-pass load, however due to anisotropy and inhomogeneity introduce more complexities in predicting failure modes. Their

3rd Electronic and Green Materials International Conference 2017 (EGM 2017)
AIP Conf. Proc. 1885, 020020-1–020020-8; doi: 10.1063/1.5002214
Published by AIP Publishing. 978-0-7354-1565-2/$30.00

models ignore the three-dimensional nature such as bolt bending and unsymmetrical loading effect. Among the factors which affect the strength of multi-bolt joints are the interaction of stress fields among adjacent fasteners, bolt configurations and number of bolts in a vertical or horizontal bolt lines. Godwin, Matthews and Kitty [5] conducted an experimental study of glass-reinforced plastic (GFRP) multi-bolt joints and found that vertical multi-bolts arrangement to loading direction was weaker than horizontally configurations. Experimental investigations on single-row CFRP with three-bolt joints were carried out by McCarthy and Gray [6] and found that by increasing bolt pitch equally leading to more evenly loading sharing between adjacent bolts. Similarly, as the diameter of centre bolt increased, the respective bolt able to carry higher joint load as load distribution were improved. Increasing plate-width tends to improve the load distribution balance. On the other hand, increasing clamping load in two outer bolts incline to balance the load distribution, however fatigue resistance design may not allow such unequal clamping load to different bolts in the joints.

McCarthy, McCarthy and Gilchrist [7] found that net-tension modes were susceptible to occur in multi-bolt joints due to by-pass loading transfer within adjacent bolts. It was suggested the outer bolts transfer bearing stress to adjacent bolts leading to tendency for net-tension failure to occur. Most of strength prediction works in bolted joint problems were implemented within finite element framework such as progressive damage modelling. Failure criterion and degradation law used are Hashin [8] formulation and Yamada-Sun [9] law respectively in progressive damage modelling implemented by McCarthy, McCarthy and Lawlor [10] work based on ply-by-ply basis. Three steps were implemented as follows: (i) stress analysis, (ii) implementation of failure criteria and (iii) degradation of material properties. McCarthy used homogeneous material properties based on Classical Laminate Plate Theory (CLPT) used as elastic material properties, however this theory is applicable to unidirectional composites, they also elaborate the use of proper contact interaction between bolt-hole and other contact regions. However, available CLPT theory is not applicable to woven fabric composites as there are existing crimping region. Ishikawa and Chou [11] proposed notable three classical models based on Classical Laminated Plate Theory (CLPT) of 2-D woven fabric composites that able to predict thermo-elastic properties. However, these formulations were based on micro-scale modelling known as representative volume element (RVE), complex mathematical formulations were involved as multi-scale modelling were involved leading to its impractical use.

Current work was carried out to implement a 3-dimensional finite element approach to predict bearing stress at failure in single-row multi-bolted woven fabric kenaf composite joints. The modelling framework explicitly includes frictional loading transfer, clamping load and surface interactions by using ABAQUS CAE Version 6.13 by implementing physically-based constitutive law. Extended Finite Element Method (XFEM) were implemented which were introduced by Moes et al., [12] and was implementing in predicting bearing stress at failure in single-bolt double-lap and single lap CFRP joints [13]. XFEM is extended from classical finite element expression which has enhanced function to enable the crack be tracked visually. The strength prediction works were validated against experimental datasets, subsequently discussed in discussion section.

EXPERIMENTAL FRAMEWORKS

The experimental framework was carried out and its description on composite plate preparations, testing series investigated and mechanical testing are given in following section. The elastic and material properties used were also carried out and implemented within finite element modelling in later stage.

Testing Coupon Preparations

Fabrications of woven fabric kenaf fiber reinforced polymer (KFRP) panels were carried out at Fabrication Laboratory, Universiti Tun Hussein Onn Malaysia (UTHM). Kenaf yarn has a nominal diameter of 0.7 mm were weaved by using weaving handloom machine combined with epoxy resin (and hardener) to produce woven fabric KFRP panels. Cross-ply plain weave plate was used in current study with a stacking sequence of $(0/90)_{s.}$ The composite panels were allowed to harden for 24 hours under high pressure and visible voids were inspected.

A testing coupon has a plate width, W = 25 mm and gauge length, l = 165 mm. Plate end distance, e were fixed to normalised end distance, e/d = 4 and corresponding normalized plate width was taken as W/d = 5. 5 mm diameter circular holes were drilled according to testing series, with 23 mm pitch spacing, p were provided between adjacent holes. The fastener systems used in current joint configuration system are steel washers and steel bolts. M5 bolts and washers were installed and bolt load were applied with finger-tight and torque wrench (in case of torque, T=5 Nm)

prior to mechanical testing. Two steel washers were provided below the bolt head and above the nut to provide lateral pressures in out-of-plane direction. Figure 1 shows schematic of single-lap joint configuration used in current experimental framework. Position of Bolt 1 were placed at the far-right in both joint configurations investigated.

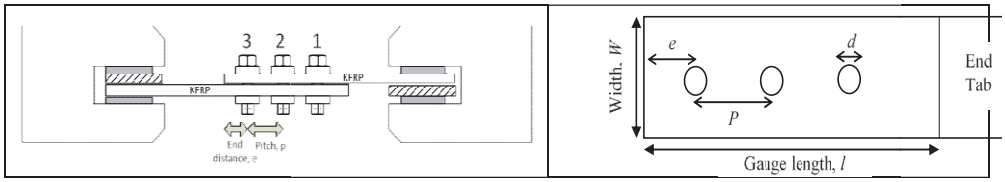

FIGURE 1. Schematic of single-lap joint configuration used in this experiment

Testing Series and Mechanical Testing

Testing series implemented in current work is given in Table 1, consisting of two or three bolts with two different clamping load respectively. The installation torques studied were a finger-tight condition (approximately equal to 0.5 Nm) and a clamping load of 5 Nm. Four bearing stresses at failure were obtained using Equation (1) and used as experimental datasets used in finite element validation stage.

TABLE 1. Testing series of experiment frameworks

Plain weave	Number of bolt in single-row	Clamping condition	Laminate designation
PX2 $(0°/90°)_s$	2 bolts	Finger-tight (0.5 Nm)	2BFT
		Torque (5 Nm)	2BT5
	3 bolts	Finger-tight (0.5 Nm)	3BFT
		Torque (5 Nm)	3BT5

$$\text{Bearing stress at failure, } \sigma_b = P_{max} / d\,t \tag{1}$$

where P_{max}, d and t are the ultimate load at failure, hole diameter and plate thickness respectively.

Mechanical testing of testing coupons was carried out under quasi-static tensile loading using an Instron Universal Testing Machine (UTM) with 100 kN load cell and crosshead speed of 0.5 mm/min, following ASTM standard D3039. Load and displacement profiles were recorded at one-second intervals using a PC data-logging package from Instron. The plate thickness was measured by using micro-meter and averaged through its gauge length.

XFEM MODELLING TECHNIQUE AND APPROACH

Three-dimensional multi-bolted models were developed in ABAQUS CAE 6.13 following experimental framework configurations, as previously described in previous section. In order to obtain fast and precise convergence, pre-processing stage played an important stage comprised of modelling idealization, meshing, generation of materials (and geometry) properties and boundary conditions. The predicted XFEM joint strength and failure modes of multi-bolted joints were then analysed and compared with experimental results.

Modelling Idealizations

The numerical models developed in the present work were half-model of three-dimensional modelling framework following experimental configurations of single-lap multi-bolt joints to reduce computational cost and time effort. The models were explicitly including frictional load transfer, bolt clamp-up and surface interaction. The bolt head, bolt shaft and nut were modelled as a single unit where the clamping load (bolt pre-tension) were implemented within internal surface of bolt shaft as suggested by ABAQUS CAE documentation. The washers were separately model to allow explicitly frictional load transfer within joining plates. Perfect fit conditions between bolt

shank and bore hole were assumed in all models to eliminate the effect of clearance, low tolerance in aerospace sector were allowed and to the lesser extent in civil engineering sector.

Generation of Materials and Geometrical Properties

The boundary conditions and applied displacements were assigned accordingly to resemble mechanical testing conditions. As described earlier, elastic properties of KFRP used in the present model were obtained from independent experimental set-up and were considered as "smeared-out" properties, given in Table 2. The unnotched strength, σ_o and fracture energy, G_c were also determined independently, both material properties were later used as constitutive model parameters described in next section. Woven fabric KFRP composites plates were modelled with nominal plate thickness of 2.1 mm.

TABLE 2. Material properties of KFRP lay-up used in current work

Lay-up	E_x (MPa)	E_y (MPa)	ν_{xy}	σ_o (MPa)	G_c (kJ/m^2)
PX2 (0°/90°)s	2260.33	2260.33	0.07	54.70	5.3

Boundary condition at far-left is held fixed and applied displacement was assigned at the far-right as shown in Figure 2. All surface interactions were modelled as "master-slave" interaction and penalty friction value were implemented with friction coefficient of 0.3 and 0.1 for composite-composite and composite-steel surfaces respectively. Master surface was assigned in materials with larger modulus and exhibited less deformable than relatively weaker joining materials (assigned with slave surface). The contact between two surfaces was modelled as small sliding and surface-to-surface as sliding formulation and discretization method respectively. Combination of small sliding and surface-to-surface discretization gives more realistic physical perturbation and cover larger contact area between contact pairs. XFEM regions were assigned within the net-tension plane at the vicinity of Bolt 1 as observed during mechanical testing. Y-symmetry was assigned at the y-axis to represent half-model configurations as idealized previously.

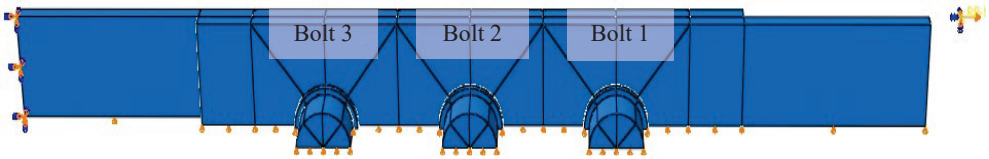

FIGURE 2. Boundary condition and loading applied of 3-D multi-bolted joints model

The mesh ahead of hole edge (particularly area under washers) were refined and remaining plate regions were made coarser to save computational effort as shown in Figure 3. Full integration method was implemented to avoid hour-glassing effect (in case of using reduced integration technique). In current study, damage stabilization value of 1 x 10^{-5} was implemented throughout all models and first-order brick elements with element designation code of C3D8I (an 8-node linear brick, incompatible modes) was used as element type. These elements were chosen as only first-order elements and brick elements were compatible in current standard ABAQUS Version 6.13 with XFEM framework. Brick elements are prone to shear locking phenomenon, however, these effect can be avoided by using incompatible modes.

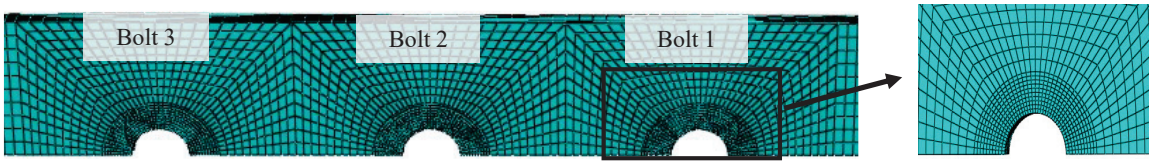

FIGURE 3. Meshing of 3-D multi-bolted joints model based on experimental plate geometry (The notch edge at Bolt 1 is enlarge for visual clarity)

Modelling Strategy using XFEM Approach

A physically-based constitutive model implemented was shown in Figure 4 based on traction-separation relationship. The maximum cohesive stress is given at the maximum separation length and equivalent to un-notched plate strength, σ_o and area under the curve is given as fracture energy values, G_c both parameters are regarded as material properties. Three points were highlighted in Fig. 4, where between Points 1 and 2, no material separation has occurred. As the separation increased, cohesive traction achieves a maximum cohesive stress as labelled in Point 2. Between Points 2 and 3, cohesive traction decreases and finally stopped at Point 3 enable complete material separation and provide energy absorption for de-cohesion.

Maximum principal stress (Maxps) was used as failure criterion which allowed the crack to propagate orthogonally to the direction of maximum principal stress. Mode independent was used due to only opening mode (Mode 1) was exhibited as observed experimentally. XFEM formulation is based on partition of unity and extended from classical finite element method is driven by energetic approach. XFEM is not sensitive to mesh refinement at the crack tip therefore it can avoid very fine mesh dependency around the crack tip as a results of stress singularity at the crack tip in classical finite element formulation. XFEM region were assigned within net-section failure path to allow crack propagation in order to allow quicker convergence.

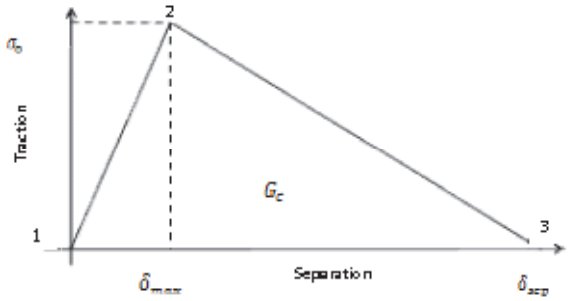

FIGURE 4. Physically-based constitutive model used in current work

RESULTS AND DISCUSSIONS

The experimental observations and validation work of XFEM models with experimental datasets were given in the following sub-sections.

Experimental Observations

All testing series were tested under quasi-static tensile loading using an Instron Universal Testing Machine (UTM) at Structure Laboratory, Universiti Tun Hussein Onn Malaysia (UTHM). The testing coupons were labelled accordingly as specified in testing series as previously described in previous section (Testing Series and Mechanical Testing). Figure 5 showed a representative testing coupon with net-tension failure mode with two and three bolts joints. All testing series coupons were showing similar trends, net-tension failure was exhibited in Bolt 1 and slightly bearing failures exhibited in other adjacent bolts. As a result of secondary bending due to unsymmetrical loading path, the plate edges were lifted and contribute to extra tensile stresses and associated with reduced loading capacity of composite plates. It was found that similar amount of plate edges lifting found on both joining plates of similar material (KFRP), as expected.

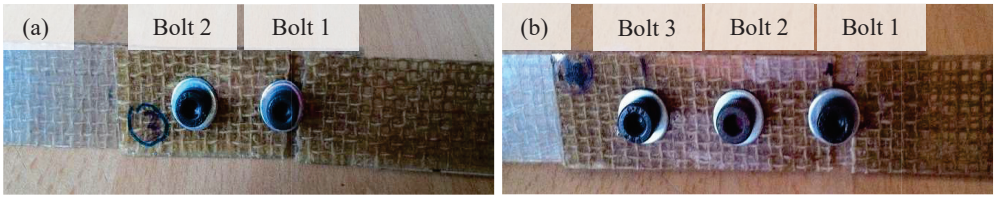

FIGURE 5. Experimental observation of testing coupons with (a) 2BT5 (b) 3BT5

Bolt pull-through was demonstrated and penetration of washer into composite plate due to bolt tilting, more prominently under clamped condition. A representative of load-displacement profile curve is shown in Figure 6. Initially the joint deformation is contributed by linear elastic of un-lapped region. At this stage, no slippage occurred as applied load, P_{app} < clamping load, P_{bolt} and the applied load is transferred genuinely through friction. Thereafter, slippage occurred at shear plane when P_{bolt} exceeds P_{app}, then the load transfer is borne by individual plates. The sliding load in Fig. 6 is given by plateau curve under slip region. Bearing contact between bolt shaft and bore hole occurred thereafter and exhibited bearing stress within bearing area, a product of hole size, d and plate thickness, t.

All testing coupons were initially demonstrated bearing deformation (associated with hole elongation) at Bolt 1. Subsequently, Bolt 2 and Bolt 3 demonstrated bearing stresses to the lesser extent, this phenomenon is prominent in finger-tight condition (where hole elongations are clearly seen). However, the ultimate failure mode is in net-tension where the crack is initiated at the vicinity of hole edge and propagated to the plate edge along net-tension plane. Net-tension failure demonstrated catastrophic failure, most research work on bolted joints favours bearing failure which gives more progressive failure manner. However, net-tension failure is unavoidable due to several constraints such as design geometry requirements and net-tension failure is more likely to occur in multi-bolted joint as a results of by-pass loading of bolts to the nearest bolts. Similar finding were reported by McCarthy, McCarthy and Gilchrist [7], where higher bearing/by-pass stresses was exhibited in Bolt 1. This leads to ultimate failure were likely to occur in Bolt 1 (similar labelling in current work are shown in Fig. 1).

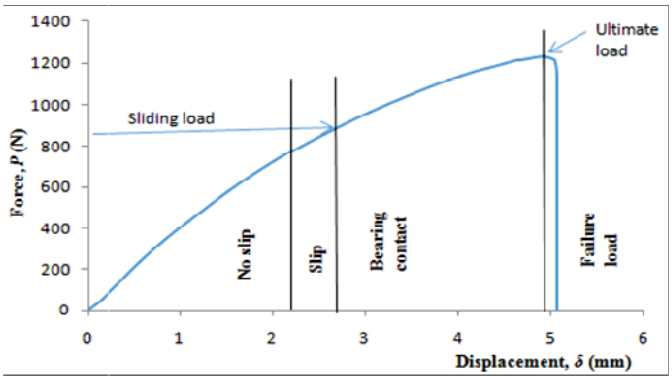

FIGURE 6. Joint behaviour of testing coupon in PX2 with 2BT5 laminate designation

Bearing Stress at Failure using XFEM Modelling

Current 3-D modelling works used 'smeared-out' elastic properties, based on independently determined in-plane properties investigated experimentally, previously mentioned in previous section (Generation of Materials and Geometrical Properties). On the other hand, out-of-plane elastic properties of KFRP woven fabric composites were determined from expression taken from Ahmad [14]. XFEM formulation able to visualise the crack formation at the vicinity of the hole edge, current approach implemented XFEM region at the vicinity within Bolt 1 as shown in Figure 7, therefore crack initiation and propagation were exhibited within these assigned regions.

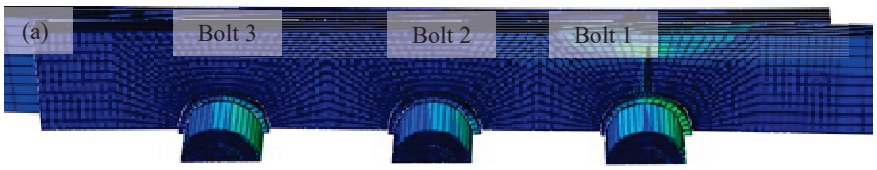

FIGURE 7. Joint behaviour of testing coupon in PX2 with 2BT5 laminate designation

Figure 8 shows a typical load-displacement curves from the XFEM modelling, a representative curve given by 2BFT series. Due to the stress concentration at the hole under tensile loading, the damage is associated with stress concentration at the hole edge. Initially, as observed experimentally the linear elastic at the early stage was contributed by un-lapped plate region. Crack initiation is exhibited at an angle approximately 85° from y-direction

as given by Point A, at this point, the damage is progressively took place. At this point, the respective plate still able to carry more load until ultimate load. Point B shows ultimate failure load from current modelling work which associated to catastrophic failure. Ultimate load is given as the crack reached about a radius of hole size. After Point B, the crack is propagated until separated completely, Point B to Point C occurred in a short period of time (catastrophic failure).

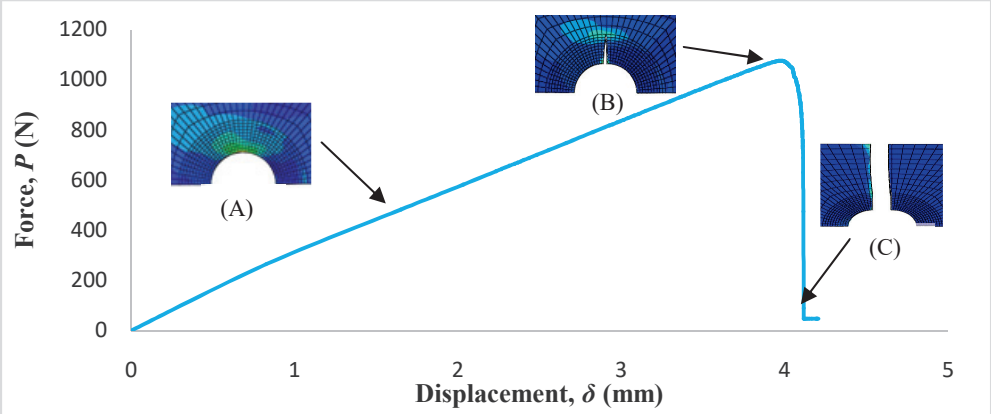

FIGURE 8. Joint behaviour of testing coupon in PX2 with 2BT5 laminate designation

Validation of XFEM Models with Experimental Datasets

Table 3 showed comparison between experimental results and strength predictions for all testing series understudied. As expected, bearing stress at failure of KFRP plates with 5 Nm bolt load showed better agreement compared to strength prediction in 2-D modelling. From Table 3, a very good agreement was found under torqued condition (both 2 bolts and 3 bolts models gives discrepancy of less than 5%). Good correlation was also found under finger-tight loading. Current model implemented 3-D modelling framework, therefore the load transfer due to friction and bolt load was physically represented. Current work used sliding load taken from load-displacement profiles which showed a slight plateau to indicate slippage of joining plates to calculate the actual (true) bolt load applied.

In 3-D modelling framework, effect from secondary bending, bolt tilting, joining plates sliding, bearing contact and applied bolt load were explicitly modelled. It is expected that effect of secondary bending is less significant in multi-bolt problem compared to single-bolt problem due to less bolt tilting in multi-hole problem leading to less edge lifting. Secondary bending effect is relying on bolt tilting and penetration of washers may exhibit on composite surface. Exhibition of secondary bending increases the tensile stress, and therefore reduce the loading capacity of respective composite plates compared to equivalent double-lap joints. Secondary bending phenomenon can be captured properly in 3-D modelling, however implementation of "smeared-out" properties is expected to give good prediction with thicker plates (Larger edge lifting than necessary may exhibited in thinner plates as secondary bending occurred if smeared out elastic properties are used).

Under torqued condition, the effect of hole elongation as remote loading applied is small compared to finger-tight condition. It is expected that better predictions are shown under torqued condition due to less hole elongation exhibited (current work used "smeared out" properties that may not represented well hole elongation, but assumptions of self-similar crack may offset the hole elongation effect.

TABLE 3. Material properties of KFRP lay-up used in current work

	Torque condition	Experimental bearing stress at failure, σ_{exp} (MPa)	XFEM predictions in 2D, $\sigma_{XFEM,\ 2D}$ (MPa)	Discrepancy (%)	XFEM predictions in 3D, $\sigma_{XFEM,\ 2D}$ (MPa)	Discrepancy (%)
2 bolts	Finger-tight	110	105	- 4.5	103	+ 6.4
	Torque	148	172	+ 16.2	144	+ 2.7
3 bolts	Finger-tight	124	132	+ 6.5	122	+ 1.6
	Torque	159	199	+ 25.2	164	- 3

*Finger-tight = 0.5 Nm
*Torque = 5 Nm

CONCLUSIONS

As expected, multi-bolted joints are prone to net-tension failure and it was in-line with analytical approach due to ability by-pass loading transfer to adjacent bolts. Good agreements were found in all testing series (less than ±10% discrepancy). Better predictions of bearing stress at failure were found under torqued case compared to previously 2-dimensional model as a result of applied bolt load is incorporated physically in the model (previous 2-D models rigorously adding sliding stress to predicted bearing stress). Moreover, 3-D modelling able to capture frictional load transfer, secondary bending and proper contact interaction (current model used "master-slave interaction" that allows penetration of slave surface onto master surface, similar physical observations under bearing after slippage occurred).

ACKNOWLEDGMENTS

The authors would like to acknowledge Universiti Tun Hussein Onn Malaysia for providing laboratory facilities and financial assistance under project Vot No. U549.

REFERENCES

1. T. Nishino, K. Hirao & M. Kotera, Composites Part A: Applied Science and Manufacturing 37, 2269–2273 (2006)
2. H. R. Anders and H. Ahmad, "Notched strength of woven fabric kenaf composite plates with different stacking sequences and hole sizes", (Matec Web of Conferences, EDP Sciences, 10.1, 2016)
3. J. H. Crews and R. A. Naik, "Combined bearing and bypass loading on a graphite/epoxy laminate", (Composite Structures, Google Scholar, 1986), pp 21-40
4. C. L. Hung and F. K. Chang, Journal of Composite Material, (1996)
5. E. W. Godwin, F. L. Matthews and P. F. Kitty, "Strength of multi-bolt joints in GRP", (Composites, Joining in fibre-reinforced plastics, 1982), pp 268-272
6. C. T. McCarthy and P. J. Gray, Composite Structures 93.2, 287–298 (2011)
7. C. T. McCarthy, M. A. McCarthy and M. D. Gilchrist, Engineering Materials 293, 591-598 (2005)
8. Z. Hashin, Journal of Applied Mechanics 47, 329-334 (1980)
9. S. E. Yamada and C. T. Sun, Journal Composite Materials 12, 275-284 (1978)
10. C. T. McCarthy, M. A. McCarthy and V. P. Lawlor, Composite Part B – Engineering 36, 290–305 (2005)
11. T. Ishikawa and T. W. Chou, Journal Material Science 17, 3211-3220 (1982)
12. N. Moës, N. Sukumar, B. Moran and T. Belytschko, "An extended finite element method (xfem) for two and three-dimensional crack modeling", (ECCOMAS, 2000)
13. H. Ahmad, Composites Part A: Applied Science and Manufacturing 66, 82-93 (2014)
14. H. Ahmad, Journal Teknologi 78, 1-7 (2016)